IN-FLIGHT GUST AND LOAD MEASUREMENTS ON AN AIRSHIP FOR MODEL-BUILDING AND COMPARISON WITH THE TRANSPORT AIRSHIP REQUIREMENTS

Reinhard Koenig and Gerhard Wulff
German Aerospace Center, Institute of Flight Research
Lilienthalplatz 7, 38108 Braunschweig, Germany

Keywords: *Airship, Gust-Loads, Model Building*

Abstract

Airships with a combination of the pressure and rigid construction principles represent a new kind of construction where loads by gusts can be important for the design. The loads by gusts are described in the Transport Airship Requirements (TAR) by an empirical equation, which determines the maximum bending moment caused by the gust. This equation was derived from experiments with rigid airships and has been modified following the experience with blimps; its validity for airships with a combination of both construction principles has jet not been proved.

To get information about the behavior of an airship in gusts with regard to the inner loads a research project has been carried out by the German Aerospace Center (DLR) and the manufacturer of the airship Zeppelin NT (Fig.1), the Zeppelin Luftschifftechnik GmbH Friedrichshafen (ZLT).

Fig. 1. Airship Zeppelin NT

The result was an extensive collection of data from measurement flights, containing the gust velocity in direction and magnitude as well as the bending moments and cross forces. Based on this data models have been developed which give information about the longitudinal bending moment caused by vertical gusts.

1 Wind velocity calculation from flight tests

1.1 Basics

Contrary to ground based wind measurement systems it is not possible to determine wind or gust speed and direction directly onboard of an aircraft/airship but they result from the difference of inertial and true airspeed [1]. In general the following vector equation is valid

wind speed = inertial speed - true airspeed

$$\underline{V}_W = \underline{V}_K - \underline{V} \qquad (1)$$

If wind determination will be performed from flight data it is useful to calculate the wind vector related to the earth fixed coordinate system. Then a simple validation will be possible, because the earth related wind components have to be independent from airship maneuvers.

$$\begin{bmatrix} u_W \\ v_W \\ w_W \end{bmatrix}_g = \begin{bmatrix} u_K \\ v_K \\ w_K \end{bmatrix}_g - \begin{bmatrix} u_a \\ v_a \\ w_a \end{bmatrix}_g \qquad (2)$$

The horizontal components of the inertial speed are available from an inertial navigation

system (INS) or a global positioning system (GPS) as north-south speed ($u_{kg} = V_{NS}$), respectively west-east speed ($v_{kg} = V_{WE}$), or have to be calculated from ground speed and true track. The vertical component is the negative rate of climb/descent (w_{kg} =-dH/dt); its determination is more complicated.

The necessary transformation of the true airspeed from the aerodynamic into the earth fixed coordinate system consists of two steps. First, a transformation from the aerodynamic to the body fixed system has to be performed using the angle of attack α and the angle of sideslip β. Then, the knowledge of the three Euler angles pitch θ, roll ϕ and heading ψ is needed to transform from the body to the earth fixed system (Fig. 2).

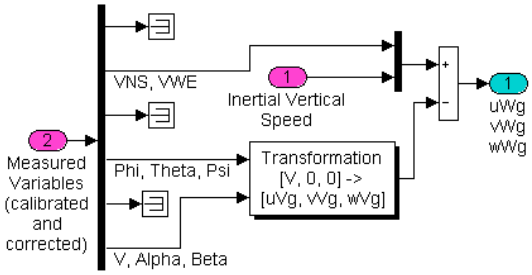

Fig. 2. Wind determination from the inertial speed and the true airspeed

1.2 Determination of the inertial vertical speed

In general, the direct measurement of the inertial vertical speed with sufficient precision and dynamic behavior is impossible. A simple differentiation of the barometric altitude can not be made, because there is normally a signal delay and an insufficient resolution. A suitable signal can be generated only by a Luenberger-Observer or a complementary filtering. The Luenberger-Observer integrates two times the earth fixed vertical acceleration and compares the result with the barometric altitude. The error is feed back, the inertial vertical speed is the output of the first integrator. The complementary filtering (Fig. 3) combines the barometric altitude after a differentiation and the earth fixed vertical acceleration after an integration.

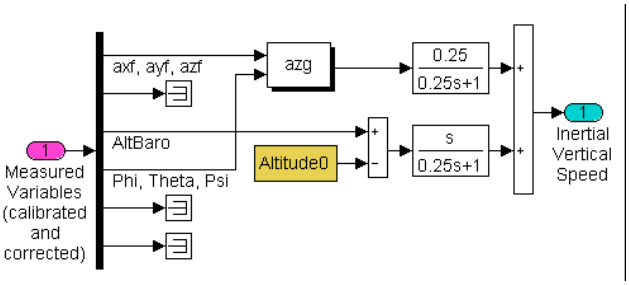

Fig. 3. Complementary filtering to determine the inertial vertical speed

1.3 Signal calibration and correction

Measurements of the true airspeed, the angle of attack and the angle of sideslip is done by a five hole probe, which is located on a nose boom in front of the gondola (Fig. 4).

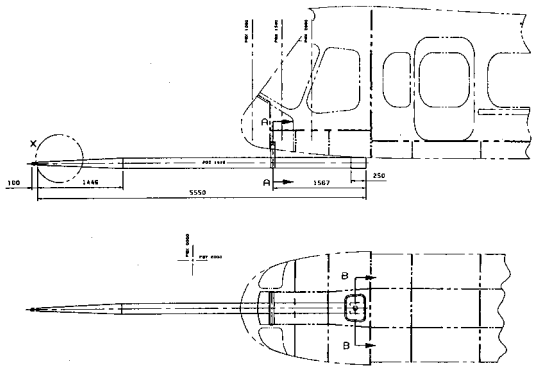

Fig. 4. Nose boom with five hole probe

This location is chosen because of a small influence of the airship body to the airflow. However, the large distance between the center of gravity and the five hole probe produces airflow resulting from rotations, which have to be corrected (Fig. 5).

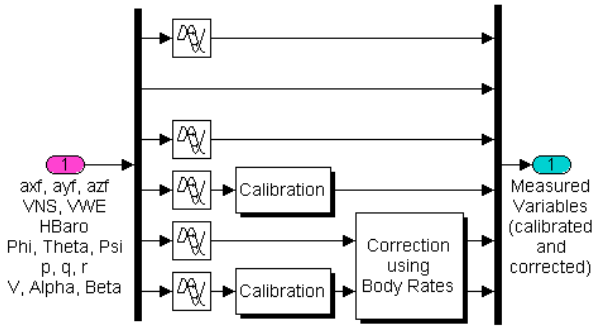

Fig. 5. Signal calibration and correction

Furthermore, correct wind determination needs all subsignals at the same time. The inertial sig-

nals from the GPS have in general a time delay. To guarantee the same time all other signals have to be delayed. The time delay can be estimated from turns whereas the calculated wind components must be constant.

Therefore the wind determination contains subsequent signal processing, calculation of the inertial vertical speed and transformation of the true airspeed into the earth fixed coordinate system (Fig. 6).

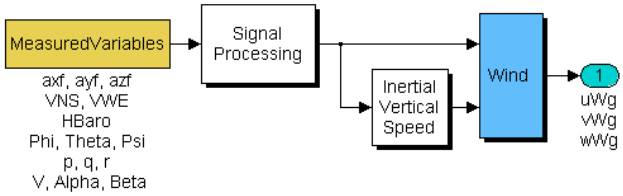

Fig. 6. Wind determination

1.4 Methods to validate the wind determination

Actually a validation of the wind determination needs a comparison with an independent separate wind measurement. This is only possible by flying past ground based wind measurement stations or formation flights together with an aircraft/airship equipped with a validated wind measurement system. Supposing that the true wind speed remains constant during a flight maneuver, statements about validity and precision can be made. Such maneuvers are horizontal flight-path reverse, stimulation of the airship dynamic behavior and turns [2]. The basic idea is, that the calculated wind speed must be independent from any flight maneuvers. Then, from obvious errors in the wind determination, errors in the measurement data processing, errors in the calibration, or biased errors in the measured variables can be detected and corrected. A definite allocation can be very difficult sometimes.

2 Considerations about the validity of a stationary gust field

Gusts alter with position and time. The displacement with the mean wind leads to the fact that a gust changes the position. If the gust shape alters with the time, one speaks of an instationary change. Both changes can be usually neglected if an airplane crosses the gust, since on the one hand the true airspeed of an airplane is high and on the other hand the airplane dimensions are relatively small. That means, one can assume the gust does not alter its shape during the aircraft's crossing.

On the example of the gust alleviation system LARS of the experimental aircraft ATTAS of the DLR the described assumption shall be illustrated again [3]. For a gust alleviation the gust is measured and suitable control surfaces at the airplane are deflected in such a way that the undesirable gust reactions are reduced. The gust effects mainly on the wing, but it is measured at a nose boom before the airplane, in order to keep off any influences on the airflow from the fuselage. The assumption that the gust between measurement and effect does not change, could be confirmed by the flight tests, because the gust reduction system was effective. At a true airspeed of 70 m/s and a distance from the nose boom to the wing of approx. 12 m, the time between measurement and effect is about 0,17 seconds.

Conditions at an airship are looking there somewhat different. Small airspeeds (Zeppelin NT: 32 m/s) and large dimensions (distance between nose and center of gravity approx. 38 m) lead to more than one second of diving into the gust. Within this time cannot be any longer absolutely assumed that the gust is stationary. However the gust effect is no longer limited within wing location. The gust works over the entire immersed body. The airworthiness directives for airships assume the half airship length as the smallest wavelength of a 1-cos gust. This gust leads to a maximum bending moment near the center of gravity, if the point of attack of the resulting aerodynamic force is located at 25% airship length from the nose. A measurement of the flow vector within this area defuses the problem, which temporally instationary gusts bring with itself, substantially. In this area is the gondola, and the mounting of a flow probe at a nose boom is possible and was executed.

Instationary gusts represent a secondary problem when between measurement and maximum effect only a short time elapses, i.e. when measuring point and point of impact are

sufficient close together. Only several measuring points of the flow vector can give certainty referenced to this statement, which however within this project was not realizable. Further knowledge to this topic could be derived also from the time response of the bending moment measured at different longitudinal positions.

3 Measurement of the internal loads

During the assemblage of the first airship LZ N07, segment 6, which is the segment of the carrying structure directly behind the gondola, and segment 10, which is the segment in the area of the empennage, were armed with strain gauges due to measure in-flight the internal loads [4]. In segment 6 all three longerons are provided with strain gauges in the middle and at the end (Fig. 7). All with strain gauges equipped components were calibrated in a test equipment before installation and the offsets of the measuring points were determined.

After structure assemblage pre-loading occurs and the offset-values are no more valid with sufficient reliability. Therefore an exactly defined zero load-case was generated with the complete structure of the airship. On this basis the internal loads then were determined finally. The influence of the hull, which is carrying a non negligible part of the loads, originally is not contained in the measured values. During calibration tests with the assembled airship, with and without hull, defined cross forces were applied in z-direction. Then the computing procedure was finally adapted in such a way for the determination of the internal loads, that also the influence of the hull is considered.

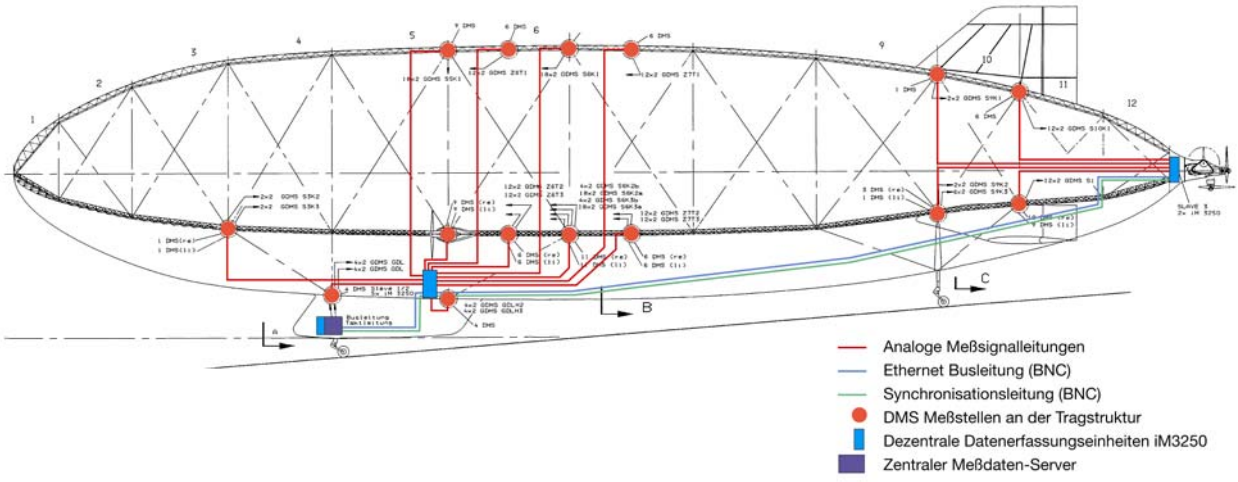

Fig. 7. Flight test measurement system and location of the structure measurement points

4 Aerodynamic bending moment from TAR

For the structural design of an airship the loads by gusts can be relevant. For this reason the transport airship requirements (TAR) [5] contain an equation of the aerodynamic bending moment due to a given 1-cos gust, which has to be taken into account in the case of an absence of a more rational analysis by the manufacturer. The equation presents itself as follows

$$(3)\quad M = 0.058\, V \left(\frac{L}{2}\right)^{\frac{1}{4}} \left[1 + (f-4)\left(0.5624\, L^{0.02} - \frac{1}{2}\right)\right] q \frac{U_m}{v}\ [\text{lb ft}]$$

No dynamic response is calculated, only the maximum value of the bending moment is given. Gust shape and wavelength have thereby no influence. The maximum bending moment results from the maximum wind velocity U_m as well as from the airship external dimensions, like overall length L, diameter D and volume V,

and flight parameters, like airspeed v. The tables 1-3 contain the appropriate values for the Zeppelin NT.

Overall Length, L	246.1 ft
Max. Hull Diameter, D	46.6 ft
Envelope Volume, V	290 500 cu ft

Tab 1. External dimensions Zeppelin NT

Gust Speed, U_m	25 ft/s	7.62 m/s
Cruise Speed, v=V_H	118 ft/s	36 m/s
Maximum Bending Moment, M_b	2.29e+5 lb ft	**3.11e+5 Nm**

Tab. 2 Maximum bending moment related to cruise speed

Max Gust Spd., U_m	35 ft/s	10.7 m/s
Airspeed v=V_B	65.6 ft/s	23.4 m/s
Maximum Bending Moment, M_b	1.78e+5 lb ft	**2.42e+5 Nm**

Tab 3. Maximum bending moment related to maximum gust speed

Since the maximum bending moment related to the cruise speed is larger than related to the maximum gust speed, this value is relevant for the design and should be used in the comparison of measurements and simulations.

5 Bending moments and wind speeds from flight test data

During altogether 4 flights (35 flight segments) with the Zeppelin NT in July 1999, data were recorded for wind calculation and load determination at structure segment Z6 [4]. The flights were carried out with different turbulence / gust conditions and different pilot strategies, like stabilization around pitch and/or yaw axis and without any stabilization. Contrary to an airplane, which stabilizes in general after a gust transition automatically, an airship can be returned into a stable straight flight only by pilot inputs. Without pilot inputs airships change after gust effects into turns. Therefore, the measured loads result from both, the elevator and rudder deflections and the gusts, whereby a separation of the influences can not easily be performed.

In Fig. 8 the vertical wind in the body-fixed coordinate system and the measured cross forces and bending moments in structure segment Z6 of the airship are shown for the flight segment "56". Already the time response shows a clear dependency of the bending moment M_y on vertical wind.

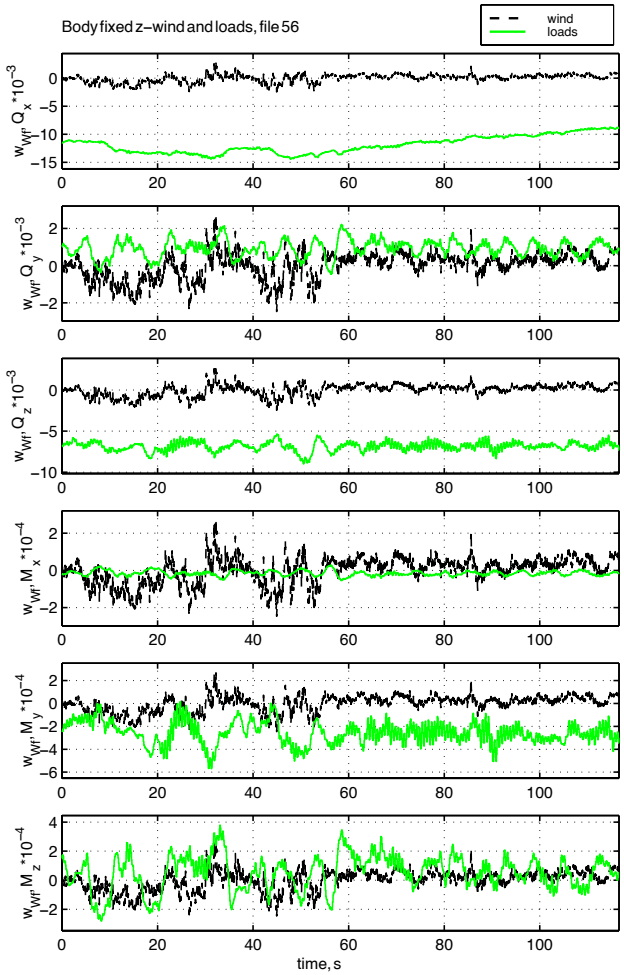

Fig. 8. Vertical wind component and loads

The power density spectra (Fig. 9) of this wind component is comparable with the Dryden spectrum. The distinctive eigen frequencies unfortunately could not be reconstructed theoretically.

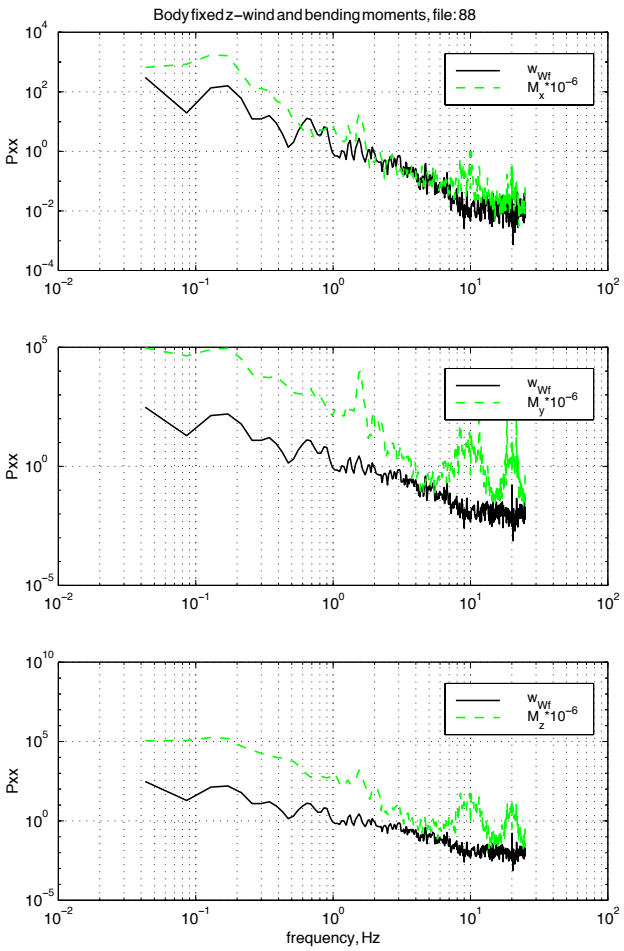

Fig. 9. Power density spectra of vertical wind and bending moments (flight segment 88)

Airspeed and flight altitude determine the dynamic pressure and thus decisively the aerodynamic bending moment. The flight tests were executed with two different true airspeeds, a mean value of 22.4 m/s, which approximately corresponds to the airspeed for maximum gust strength (V_B = 23,4 m/s), and with 30.3 m/s, somewhat lower than the cruising speed (V_H = 36 m/s). For the lower airspeed 27 (group 1) and for the higher 8 flight segments are present (group 2). The average values for the mean values, standard deviations and minima / maxima of airspeed, vertical wind, elevator deflection, pitching rate and bending moment around the y-axis are laid on in Table 4.

The mean values of the bending moment M_y vary within a wide range, the average over all mean values is negative and amounts to -1.79e+4. Also the standard deviations alter very strongly over the flight segments, which is due to the different intensity of the turbulence and due to the different elevator activities. Regarding the minima and maxima it can be stated that they deviate only few from their average values. Max. bending moment arises significantly with higher airspeed (Table 4, group 2). An influence of the altitude, whose average values were situated between 800 and 1100 m, could not be constituted.

	Mean Values	Standard Deviation	Minima Maxima
True Airspeed (Group 1)	**22.4 m/s**	1.03 m/s (1 and 2)	21.4 m/s 27.1 m/s (1 and 2)
True Airspeed (Group 2)	**30.3 m/s**		
Vertical Wind	-0.22 m/s	0.99 m/s	-3.84 m/s +2.85 m/s
Elevator	2.75 °	5.39 °	-14.3 ° +20.1 °
Pitch Rate	0.01 °/s 0.61 °/s*	0.79 °/s	-14.3 °/s +20.1 °/s
Bending M. (Group 1)	-1.79e+4 (1 and 2)	1.44e+4 (1 and 2)	**-5.77e+4 +2.10e+4**
Bending M. (Group 2)			**-7.66e+4 +4.78e+4**

Tab 4. Mean values, standard deviations and minima/maxima from 35 flight segments
* indicates turns

The largest bending moment amounts to -1.02e+5 Nm which is 33% of the load from the permission formula (see Tab. 2). It appears in flight segment 88, which indicates the largest elevator activity and the second highest standard deviations of the vertical wind and the pitch rate.

6 Transfer function between vertical wind and bending moment around the y-axis

6.1 Analyses in the time domain

On condition that during the measurement flights gust speeds of 7.62 m/s would have occurred by true airspeeds of 36 m/s (see table 2)

together with gusts of 1-cos shapes and different wavelengths from 37.51 m to 487,68 m, i.e. transit flight times from 1.04 s to 13,56 s, the measured bending moments could be compared directly with the bending moment from the TAR. Such boundary conditions are naturally difficult to find, gust wavelengths of approx. 500 m and such large gust speeds are indeed impossible. The maximum measured updraft amounts to 3.84 m/s, which is 50% of the relevant gust equation value. Of course one could come at least into the proximity of these boundary conditions for a direct comparison flying over cooling towers, but they would not be completely fulfilled thereby. It remains therefore indispensable to build up from the measured data models and to feed in during a simulation the prescribed inputs using the required magnitude and frequency from the TAR.

The measured bending moment M_y is the result of several inputs, i.e. the vertical wind, the averaged elevator deflections and the pitching rate. The model searched should contain however only the transfer function of the vertical wind on the bending moment. It will be therefore necessary to make a separation of the inputs which is possible under the prerequisite of a linear transfer function both in the frequency and in the time domain. By means of multi-input / single output analysis this is executed in [7] in the frequency domain; the results will be discussed later. For a parameter identification in the time domain one proceeds as follows.

The three inputs mentioned are given on three linear transfer blocks, whose denominators are equal and whose numerators are different. The outputs are added and formed the model bending moment, which can be compared with the measured bending moment (Fig. 10).

An optimizer adapts now the parameters of the three transfer functions (polynomial coefficients) in such a manner that the difference from model response and measured response becomes a minimum. Before comparison the measured bending moment is released from its average value and referred to the dynamic pressure. The best adjustments were achieved with a numerator degree of 2 and a denominator degree of 4 (Fig. 11).

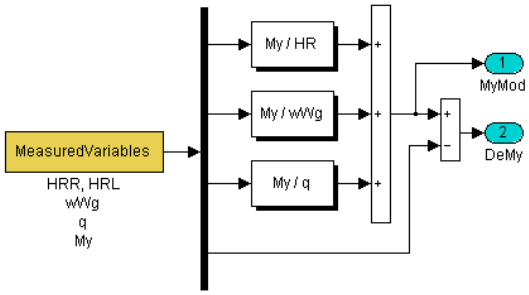

Fig. 10. Transfer functions of bending moment

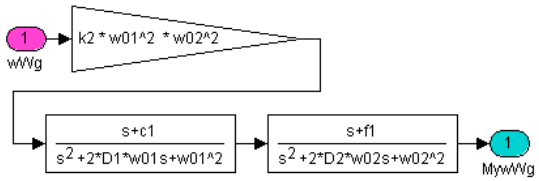

Fig. 11. Transfer function vertical wind on bending moment

Fig. 12 shows a comparison of model response and measurement in the time domain; in Fig. 13 the Bode diagram of the model is represented. The time responses fit quite well together and in the Bode diagram an eigen frequency with small damping can be regarded at 1 Hz, as also already evident from the power density spectra (Fig. 9).

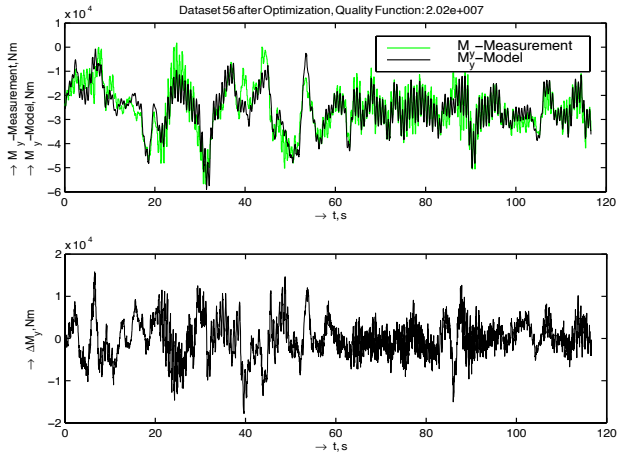

Fig. 12. Comparison between time domain approximated model response and measured response due to vertical gusts

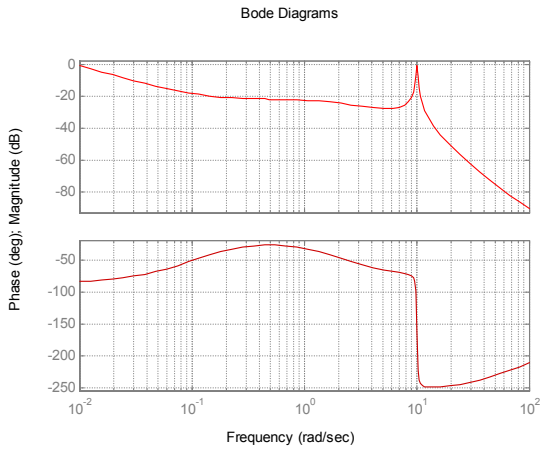

Fig. 13. Magnitude and phase of approximated transfer function

6.2 Analysis in the frequency domain

Besides of time domain also in frequency domain model building is possible and executed in [7]. Using multi-input / multi-output analysis frequency responses separated for several inputs are determined and then approximated. In difference to the time domain an averaging of the frequency dependent data takes place before the model building, i.e. there is only one model, which represents an optimal adjustment of all flight segments. Contrary in the time domain there are optimal model parameters for each flight segment and the results of the simulation are averaged.

For the investigation of the transfer function of the wind velocity on the longitudinal bending moment a lot of computations was done with XDIVA [8]. The 35 files ZEPNT56, ..., 90 of flight test data contain the input signals

δ_{SR} = rudder deflection in degree,
δ_{HRR} = elevator deflection right in degree,
δ_{HRL} = elevator deflection left in degree,
w_{Wg} = wind velocity in m/s,

and the output signals

r = yaw velocity in degree/s,
q = pitch velocity in degree/s,
p = roll velocity in degree/s,
a_{zf} = acceleration in y-direction in m/s^2,
M_y = bending moment in y-direction.

For reduction of the number of computations the signals δ_{HRR} and δ_{HRL} have been joined to the new signal $\delta_{HR} = (\delta_{Hrr} + \delta_{HRL})/2$.

6.2.1 Power spectra and energy

The power spectra $S_{ii}(f)$ of nearly all the signals mentioned above contain 100 percent of energy at frequencies less than f = 1 Hz, but the signal M_y shows at the frequency f = 1.6 Hz still a part of energy which cannot be neglected.

6.2.2 Frequency response and coherence functions

In the case that the inputs $X_1(f), X_2(f)$, ... of a linear system are correlated, their frequency response functions $H_{1y}(f)$, $H_{2y}(f)$, ... to the output $Y(f)$ can be computed as follows: First, a MISO system with conditioned second input is considered. The first input $X_1(f)$, which should have a stronger coherence to the output $Y(f)$ as all other inputs, is used unchanged with the transfer function $L_{1y} = S_{1y}/S_{11}$, but the linear parts of X_1 in the input X_2 (with the second largest coherence to Y) are subtracted from X_2 (conditioning) $X_{2.1!} = X_2 - L_{12}X_1$ with $L_{12} = S_{12}/S_{11}$.

The conditioned input spectrum is $S_{22.1!} = S_{22}(1-\gamma_{12}^2)$, the conditioned output spectrum is computed as $S_{yy.1!} = S_{yy}(1-\gamma_{1y}^2)$, and the conditioned cross-spectrum is $S_{2y.1!} = S_{2y} - L_{1y}S_{21}$. From the spectra the partial coherence function is computed as $\gamma_{2y.1!}^2 = |S_{2y.1!}|^2/(S_{22.1!}S_{yy.1!})$ and the frequency response function from the conditioned input to the conditioned output as $L_{2y} = S_{2y.1!}/S_{22.1!}$. The multiple coherence function $\gamma_{y:x}^2 = 1-(1-\gamma_{1y}^2)(1-\gamma_{2y.1!}^2)$ is a measure for the quality of the model. In the case that the multiple coherence function doesn't take values near 1, as it is in our flight test data, another conditioned input $X_{3.2!}$ should be used, in our case this is the signal q. The transfer functions of interest are then

$H_{3y} = L_{3y}$
$H_{2y} = L_{2y} - L_{23}H_{3y}$
$H_{1y} = L_{1y} - L_{12}H_{2y} - L_{13}H_{3y}$

6.2.4 Frequency response approximations

It turned out that the three frequency responses $H_{14} = M_y / \delta_{HR}, H_{24} = M_y / w_{Wg}, H_{34} = M_y / q$ computed from some experiments can bee approximated simultaneously by a model of the form

$$H_{i4} = \frac{b_{0i} + b_{1i}s + b_{2i}s^2}{a_0 + a_1 s + a_2 s^2 + a_3 s^3} \quad (i = 1,2,3)$$

with the degree 3 of the denominator and the degrees 2, 2, 1 of the numerators. For obtaining some statistical robustness first the corresponding frequency responses have been combined by computing their arithmetic mean and the results were approximated simultaneously by the above mentioned model [7]. The result is shown in Fig. 14.

The resulting polynomial coefficients of the approximation in the frequency domain lead, when inserted into the simulation model, to a relative good fitting of the model data with the measurement results in the time domain (see Fig. 15).

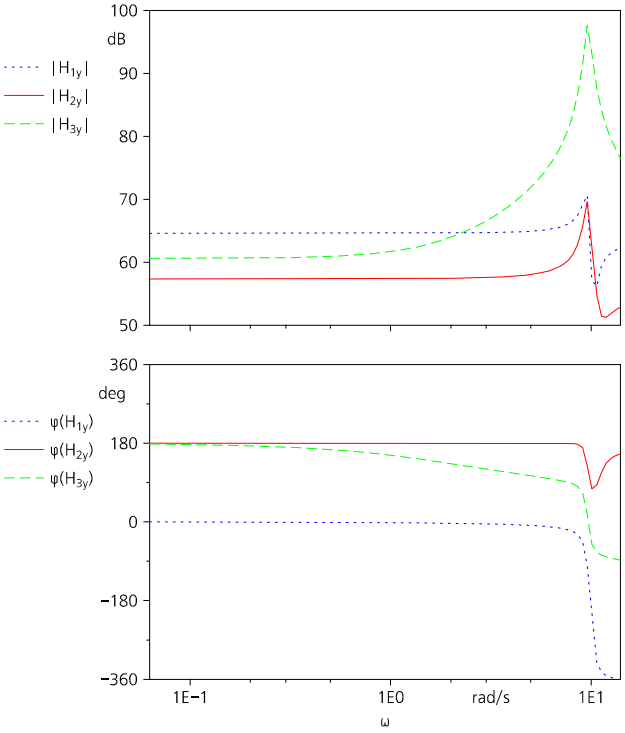

Fig. 14. Joint frequency response approximation

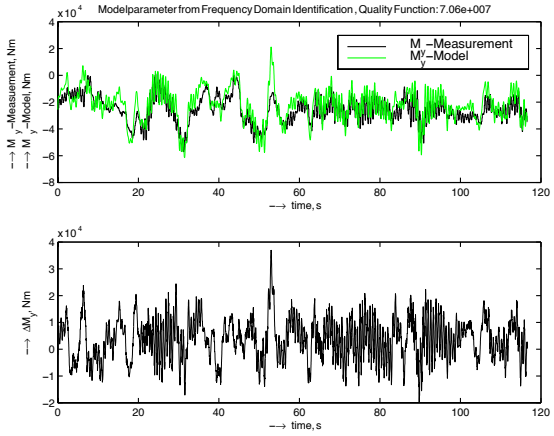

Fig. 15. Comparison between frequency domain approximated model response and measured response due to vertical gusts

7 Comparison with the TAR for a 1-cos gust input

Now after determination of the transfer function the time response of the bending moment as output signal can be calculated using input signals like 1-cos gusts according to the TAR. Furthermore a comparison of the maximum bending moment with the gust load equation is possible. The first step to approximate the transfer function was to divide the bending moment through the dynamic pressure. Before comparison it is now required to multiply with the dynamic pressure related to the decisive true airspeed from the TAR. The simulations are performed using the minimum and maximum gust wavelength. For the flight segment 56 the results are represented exemplary in the Fig. 16 and 17. With short wavelength of the 1-cos gust 38,01% of the equation value occur, with long wavelength 72,91%. Further Fig. 16 shows a small damped eigen frequency due to the relative high frequently stimulation.

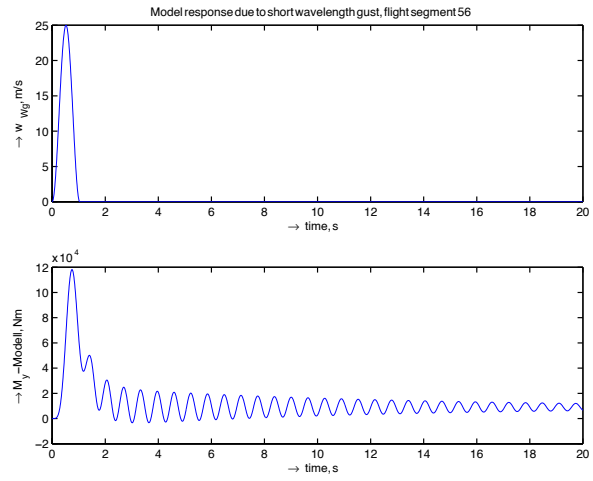

Fig. 16. Time response of the bending moment M_y for gust input with short wavelength

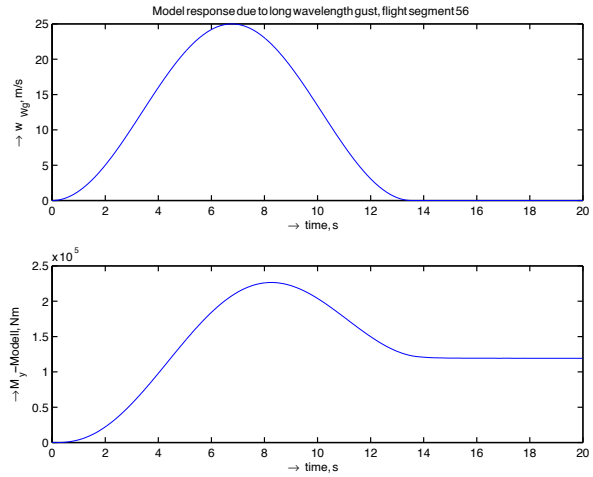

Fig. 17. Time response of the bending moment M_y for gust input with long wavelength

The maximum bending moment M_y is in both cases considerably below the gust load equation's value; therefore a calculation using the formula can be regarded as on the safe side. But this statement cannot be met however for all flight segments. Fig. 18 shows the respective simulated maximum bending moment value in percent of the formula value, both for the short (PMaxMy1) and for the long gust wavelength (PMaxMy2). All values of PMaxMy1 are less than 100%, even the most below 40%. Regarding PMaxMy2 there are 6 values, which are situated over 100%. Two of it belong to turns. Since the model building presupposed a pure longitudinal movement, turns should be removed here. Then, however further 4 flight segment with a PMaxMy2 of more than 100% remain in the analysis. An evident reason for the high bending moment occurring here could not be found. The average value of PMaxMy1 amounts now to 18,98%, that by PMaxMy2 54.27%; both are considerably below 100%.

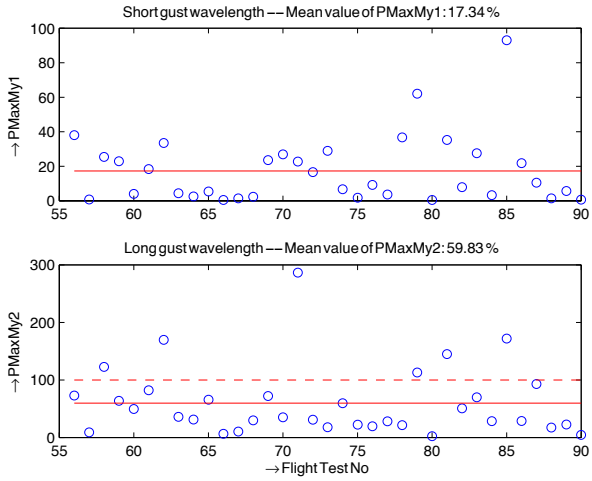

Fig. 18. Maximum bending moment from simulation for short and long gust wavelength (percentage value of gust load equation result)

Using the model from the approximation in the frequency domain, a maximum bending moment of 23.5% of the formula value occurs for the gust with short wavelength and 21.2% with long wavelength.

The result with short wavelength is consistent to that found with the model from the approximation in the time domain (24% to 19%). For long wavelength it is much lower (21% to 54%). A reason could be that during the parameter identification in the frequency domain the lower frequency range is not sufficient taken into account due to a data number limitation in the applied evaluation software.

8 Summary

For altogether 35 flight segments (70 minutes flight test time) of different turbulence / gust conditions and flight strategy the longitudinal bending moment and the vertical wind were analyzed with respect to the Transport Airship

Requirements. The TAR supposes a gust with a 1-cos shape and a certain magnitude, which of course could not be reached during the flight tests. Therefore a model building from the recorded data is necessary to simulate the longitudinal bending moment due to 1-cos gust inputs and to compare the results with the airworthiness requirements. This procedure would be also necessary, if e.g. discrete gusts and the relevant loads would be measured by flying over cooling towers, since one cannot assume also here, to find appropriate shapes and magnitudes.

A linear model building was done both in the time and in the frequency domain. The simulated maximum values of the longitudinal bending moment due to the prescribed gust input were compared with the value of the load formula. For the gust with short wavelength the averaged result amounts to approximated 19%, with the long wavelength to 54% of the formula value; whereby however 4 values are above 100%. A reason for these "runaways" could not be found, an error in the model building due to missing low-frequency information however could not be excluded. Furthermore it turned out that the model building in the time domain and frequency domain did not result into comparable models, but into comparable results by comparison with the load formula.

The represented procedure for model building is limited to linear models, which actually only are valid for small input magnitudes and in a limited frequency range. Surely instationary effects occur with short wavelengths and large magnitudes of the gust input, which are not covered by linear models. The instationary effects would reduce however the bending moments, so that one is with the linear models on the safe side. With the long wavelengths the airship would rise, e.g. with the upwind, and the additional bending moment would reach again zero. This is also not correctly covered by the derived models.

The data collection from [4] contains a lot of potential for further analyses. On the one hand further bending moments could be included and on the other hand the models could be refined.

9 References

[1] Vörsmann, P. Ein Beitrag zur bordautonomen Windmessung. Dissertation, TU Braunschweig, Institut für Flugmechanik, 1985.

[2] König, R. Kalibrierung und Validierung von On-Board Windmeßsystemen. Carl Cranz Gesellschaft, Seminar LR 1.14 "Flug unter Einwirkung von Wind und Turbulenz" Langenlebarn, Österreich, März 1994.

[3] König, R and Hahn, K-U and Winter, J. Advanced Gust Management Systems - Lessons Learned and Perspectives - . AGARD Flight Mechanics Panel Symposium, Active Control Technology: Applications and Lessons Learned, Turin, Italien, Mai 1994.

[4] König, R and Fecher, J. Schlußbericht zum Forschungsauftrag Nr. L-3/97 - 50163/97 "Böenlastmessungen an einem Luftschiff im Fluge". DLR IB 111-2000/19, Institut für Flugsystemtechnik, Braunschweig, und Zeppelin Luftschifftechnik GmbH, Friedrichshafen, Bodensee, April 2000.

[5] Transport Airship Requirements. Rijksluchtvaartdienst, The Netherlands / Luftfahrt-Bundesamt, Germany, March 2000.

[6] König, R. Ein Vergleich der Böenlasten aus der Bauvorschrift für Luftschiffe mit Messungen im Flug. DLR IB 111-2000/51, Institut für Flugsystemtechnik, Baunschweig, Dezember 2000.

[7] Wulff, G. Ermittlung des Übertragungsverhaltens von Windgeschwindigkeit auf Längsbiegemoment aus Flugversuchsdaten des Zeppelins NT. DLR IB 111-2000/08, Institut für Flugsystemtechnik, Braunschweig, Dezember 2000.

[8] Wulff, G. Dialogprogramm zur Versuchsdatenanalyse (DIVA). XDIVA-Methodenhandbuch. DLR IB 111-98/28, Institut für Flugmechanik, Braunschweig, September 1998.